Noise-induced torus bursting in the stochastic Hindmarsh-Rose neuron model

Lev Ryashko* and Evdokia Slepukhina†
Institute of Natural Sciences and Mathematics, Ural Federal University, Lenina 51, Ekaterinburg, Russia
(Received 17 April 2017; published 14 September 2017)

We study the phenomenon of noise-induced torus bursting on the base of the three-dimensional Hindmarsh-Rose neuron model forced by additive noise. We show that in the parametric zone close to the Neimark-Sacker bifurcation, where the deterministic system exhibits rapid tonic spiking oscillations, random disturbances can turn tonic spiking into bursting, which is characterized by the formation of a peculiar dynamical structure resembling that of a torus. This phenomenon is confirmed by the changes in dispersion of random trajectories as well as the power spectral density and interspike intervals statistics. In particular, we show that as noise increases, the system undergoes P and D bifurcations, transitioning from order to chaos. We ultimately characterize the transition from stochastic (tonic) spiking to bursting by stochastic sensitivity functions.

DOI: 10.1103/PhysRevE.96.032212

I. INTRODUCTION

Neurons are known to exhibit an array of different behaviors, among which oscillatory activity plays an important role. In particular, neurons can display various types of oscillations, such as tonic spiking, bursting, amplitude-modulated spiking, and mixed-mode oscillations [1–3]. Mathematical models are actively developed to describe these complex activities of the biological cell as well as possible mechanisms of transitions between them.

Since neurons may be regarded as dynamical systems, transitions between different types of neural oscillations can be studied using tools of the theory for such systems. In this regard, transitions between different types of oscillatory activity in dynamical systems are often related not only to complex bifurcations but also to the presence of specific dynamical solutions, such as canards. The classical canard [4] phenomenon explains the transition under variation of a parameter from a small-amplitude limit cycle to a large-amplitude relaxation cycle through a family of canard-type cycles. This transition happens within a narrow interval of the control parameter, whereby the phenomenon is dubbed as a canard explosion. Canards are observed in the fast-slow systems. Canard limit cycles consist of parts that go close to both the attracting and the repelling branches of fixed points of the fast subsystem. Well-known examples of planar systems displaying canards are the van der Pol oscillator [4] are the FitzHugh-Nagumo neuron model [5].

Recently, a new phenomenon related to torus canards was discovered in neuron models [6,7]. Torus canards are a three-dimensional generalization of classical two-dimensional canard solutions. As with the limit cycle canards, torus canards are observed in fast-slow systems. Limit cycle canards usually appear when the full system undergoes Hopf bifurcation, and the fast subsystem exhibits saddle-node (fold) bifurcation of equilibria. Similarly, torus canards emerge when the full system has Neimark-Sacker (torus) bifurcation, and the fast subsystem undergoes saddle-node (fold) bifurcation of limit cycles [7]. The torus canard solutions spend a long time near both the attracting and the repelling branches of the limit cycles of the fast subsystem.

The torus canard phenomenon was first discovered in a model of neural activity of the Purkinje cell [6], consisting of five ordinary differential equations based on the Hodgkin-Huxley model [8]. Torus canards were recently identified [7] in other neuron models, such as the Hindmarsh-Rose-type model, Morris-Lecar-Terman equations, and the Wilson-Cowan-Izhikevich system. It was shown that in these models, torus canards emerge in the zone of transition from the rapid spiking regime to the bursting one. Benes *et al.* [9] proposed an elementary model of torus canards: a three-dimensional van der Pol–type system, in which the torus canards are rotated versions of the limit cycle canards of a planar system.

Torus canards in neuron models are associated with the emergence of bursting activity, where bursts are formed by a torus dynamical structure. In this paper, we show that such bursting can be induced by noise in the parametric zone where the deterministic system exhibits only spiking oscillations. As a basic example, we use the three-dimensional Hindmarsh-Rose (HR) model [10].

The HR model is known to exhibit rich dynamics [11–14] including bursting [12,15,16]. Several studies on the HR model have also considered chaotic transitions between spiking and bursting solutions [11,17]. Bifurcation scenarios underlying the irregular or chaotic spiking and bursting were analyzed in [18]. Mixed-mode bursting oscillations and limit cycle canards were discussed in [19]. Moreover, it was recently shown that the HR model can also exhibit torus canards and bursting [7].

As in a living system, neurons are susceptible to random disturbances. Accordingly, the study of phenomena related to the influence of noise on neuronal models is of considerable interest, particularly in light of the potential structuring effects borne by noise. It has indeed been reported that noise can induce a wide range of complex phenomena in neuron models: coherence resonance [20–22], stochastic resonance [23,24], noise-induced bursting [25–28], stochastic generation of large-amplitude oscillations [22,29], noise-induced suppression of firing [30], noise-induced chaos and order [28,31], stochastic oscillating bistability in the zone of canard limit cycles [32], etc.

*Author to whom all correspondence should be addressed: lev.ryashko@urfu.ru
†evdokia.slepukhina@urfu.ru

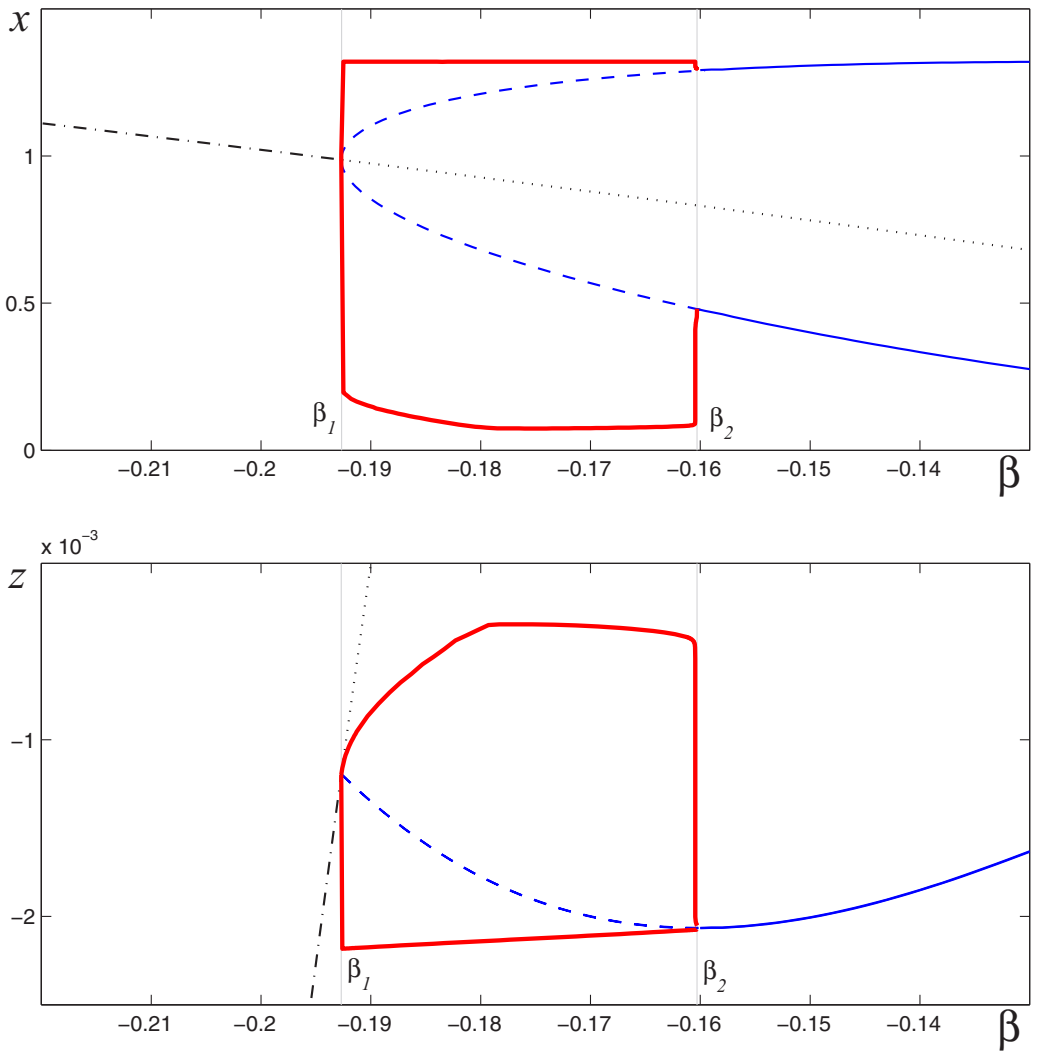

FIG. 1. Bifurcation diagram: stable (black dash-dotted line) and unstable (black dotted line) equilibria, maximal and minimal values of x (z) coordinates along stable (blue solid) and unstable (blue dashed line) limit cycles, and maximal and minimal values of x (z) coordinates along invariant tori (red thick solid line).

In this paper, we study a new phenomenon observed in the neuron model, namely noise-induced torus bursting. We show that in the parametric zone close to the Neimark-Sacker bifurcation, where the HR system exhibits rapid spiking oscillations, random disturbances can transform the spiking regime to a torus bursting one.

For a quantitative analysis of this phenomenon, we suggest an approach based on the stochastic sensitivity function technique, confidence domains, and Mahalanobis distance methods [29,30,33,34]. The stochastic sensitivity function allows us to approximate a probability density distribution of random states in the stochastic attractor. This distribution can be geometrically described by a confidence domain (an ellipsoid for an equilibrium and a torus for a limit cycle). For an analysis of noise-induced phenomena, an appropriate measure is needed for the distance from an attractor to a boundary separating basins of attraction. For this purpose, the Mahalanobis distance [30,35] can be used, insofar as this distance is proportional to the probability of escape from a basin of attraction.

The noise-induced transition from tonic spiking to torus bursting can be considered as a stochastic bifurcation. Traditionally two types of stochastic bifurcations are distinguished [36]. The first, called D bifurcation, occurs when dynamical peculiarities of stochastic flows in the system are qualitatively changed. Usually, a study of D bifurcations is based on the analysis of Lyapunov exponents. Another type of bifurcation, called P bifurcation, is connected to qualitative changes of the stationary probability density function (PDF) for the distribution of random states. In this study, we show that noise-induced torus bursting in the HR model is accompanied by both D and P bifurcations.

The present paper is organized as follows. Section II discusses the essential features of the deterministic dynamics of the Hindmarsh-Rose model in the parametric zone of quasiperiodic oscillations. In Sec. III, we describe the phenomenon of noise-induced torus bursting by direct numerical simulations of solutions of the stochastic Hindmarsh-Rose model. In the same section, we also study the probabilistic distribution of random trajectories under a variation of noise

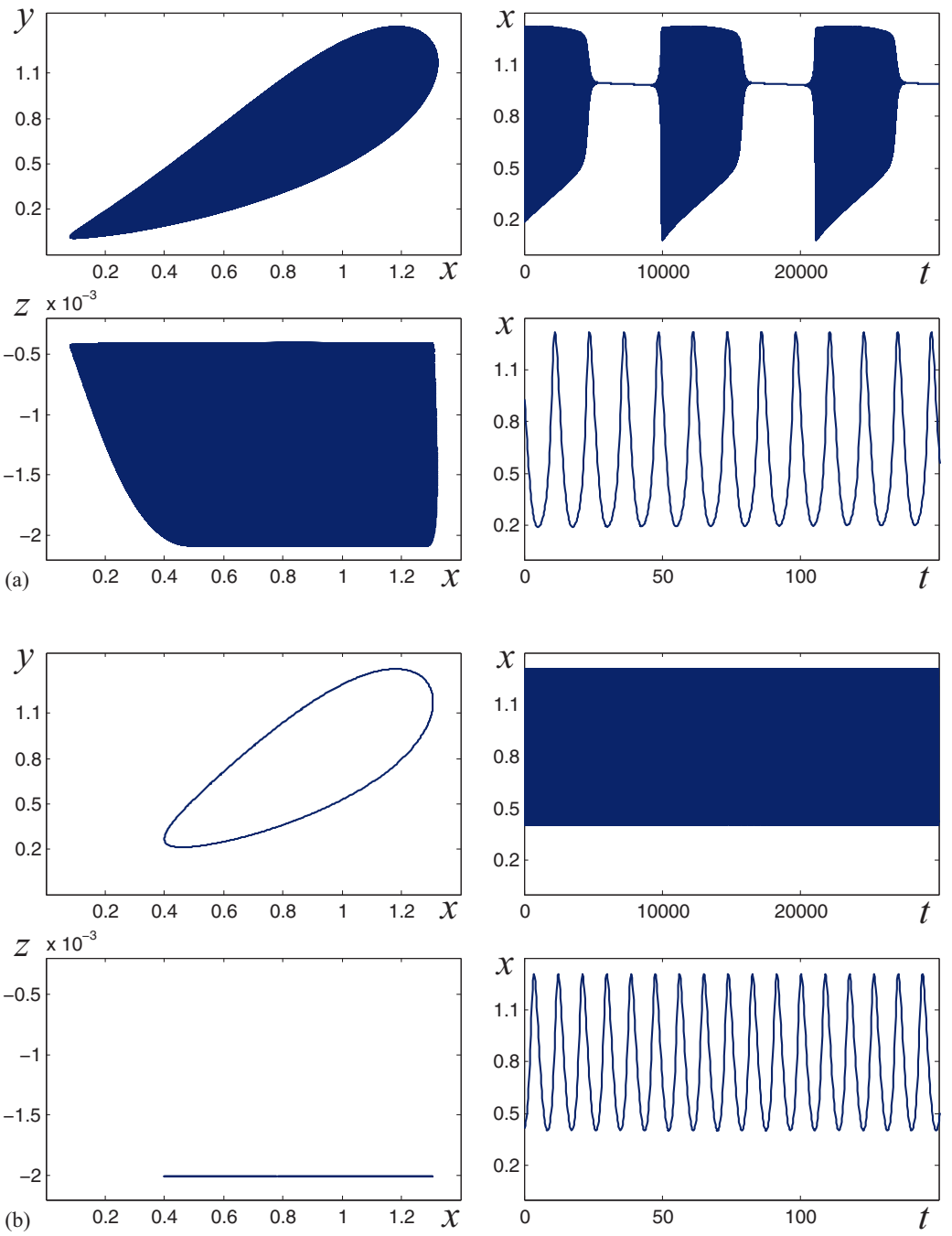

FIG. 2. Deterministic trajectories (in projection on the xOy the xOz planes) and corresponding time series $x(t)$ for (a) $\beta = -0.162$ and (b) $\beta = -0.15$.

intensity, as well as the power spectral density and the interspike interval statistics. The presence of P and D stochastic bifurcations is also discussed here. Finally, in Sec. IV we provide a characterization of this phenomenon based on the stochastic sensitivity function technique.

II. DETERMINISTIC HINDMARSH-ROSE MODEL

Consider the Hindmarsh-Rose (HR) model in the form [10,16]

$$\dot{x} = sax^3 - sx^2 - y - bz,$$
$$\dot{y} = \varphi(x^2 - y),$$
$$\dot{z} = r(s\alpha x + \beta - kz), \quad (1)$$

where x is a membrane potential; y is a gating variable; z is a recovery variable; and $a, b, k, r, s, \alpha, \beta, \varphi$ are the parameters of the system. The small parameter r $(0 < r \ll 1)$ controls the separation of time scales.

Following [7], we set $a = 0.5, b = 10, k = 0.2, s = -1.95, \alpha = -0.1, \varphi = 1, r = 10^{-5}$, and we study the dynamics of the system (1) for variations of the parameter β.

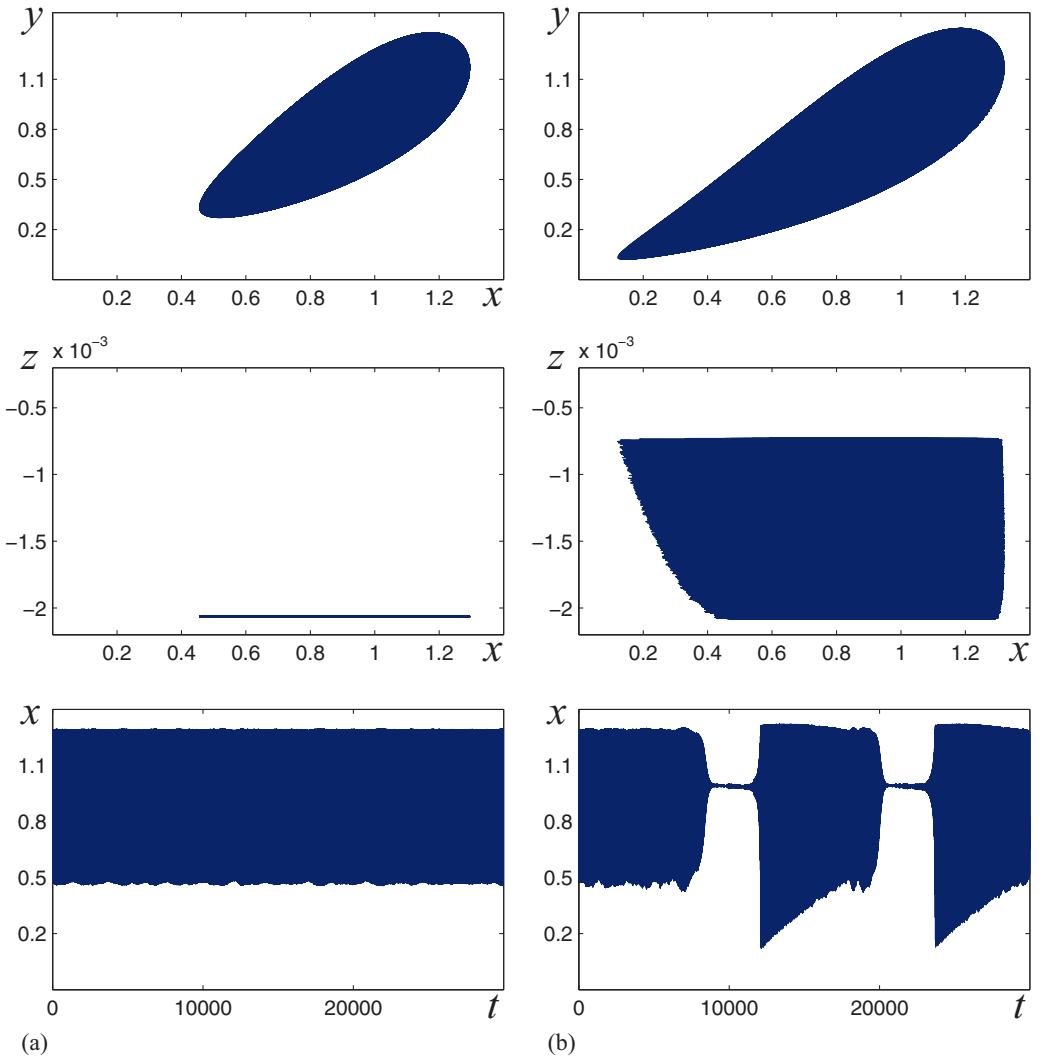

FIG. 3. Stochastic trajectories (in projection on the xOy and xOz planes) and corresponding time series $x(t)$ for $\beta = -0.159$: (a) $\varepsilon = 0.0001$, (b) $\varepsilon = 0.0004$.

Figure 1 shows the bifurcation diagram of the deterministic system (1) in the zone $\beta \in (-0.22, -0.13)$. For $\beta < \beta_1 \approx -0.1927$, the system possesses a stable equilibrium. As β increases, the equilibrium loses stability via the supercritical Andronov-Hopf bifurcation at $\beta = \beta_1$, resulting in the emergence of a stable limit cycle. The limit cycle remains stable in a very narrow parameter region: near the Andronov-Hopf bifurcation, the Neimark-Sacker bifurcation occurs with the generation of an invariant torus. Stable tori exist in the system for $-0.1927 \lesssim \beta < \beta_2 \approx -0.1603$. As the parameter passes the point $\beta = \beta_2$, the second Neimark-Sacker bifurcation occurs, and for $\beta > \beta_2$ the stable limit cycle becomes the only attractor. The transition from limit cycles to the torus near the bifurcation point $\beta = \beta_2$ is accompanied by the torus canard explosion [7].

The torus in the zone $\beta_1 < \beta < \beta_2$ of model (1) describes a special type of bursting oscillations, whereas the limit cycles in the zone $\beta > \beta_2$ reproduce the rapid tonic spiking behavior. Examples of both oscillatory regimes are shown in Fig. 2 for $\beta = -0.162$ (torus, bursting) and $\beta = -0.15$ (limit cycle, tonic spiking). In the case of torus bursting, one can observe an alternation of intervals of rapid spiking with long quiescent phases [see Fig. 2(a)], whereas in the tonic spiking regime, spikes are generated continuously [see Fig. 2(b)].

III. STOCHASTIC SYSTEM: NOISE-INDUCED TORUS BURSTING

Consider the stochastic variant of the model (1):

$$\begin{aligned} \dot{x} &= sax^3 - sx^2 - y - bz + \varepsilon\xi(t), \\ \dot{y} &= \varphi(x^2 - y), \\ \dot{z} &= r(s\alpha x + \beta - kz), \end{aligned} \tag{2}$$

where $\xi(t)$ is a standard uncorrelated white Gaussian noise with parameters $\langle \xi(t) \rangle = 0$, $\langle \xi(t)\xi^{\top}(t+\tau) \rangle = \delta(\tau)$, and ε sets the noise intensity.

In what follows, we focus on the parameter zone $\beta > \beta_2 \approx -0.1603$, where the deterministic system (1) exhibits tonic spiking (see Fig. 1).

First, consider the value $\beta = -0.159$. Here, the limit cycle is the attractor of the deterministic system (1). Figure 3 shows

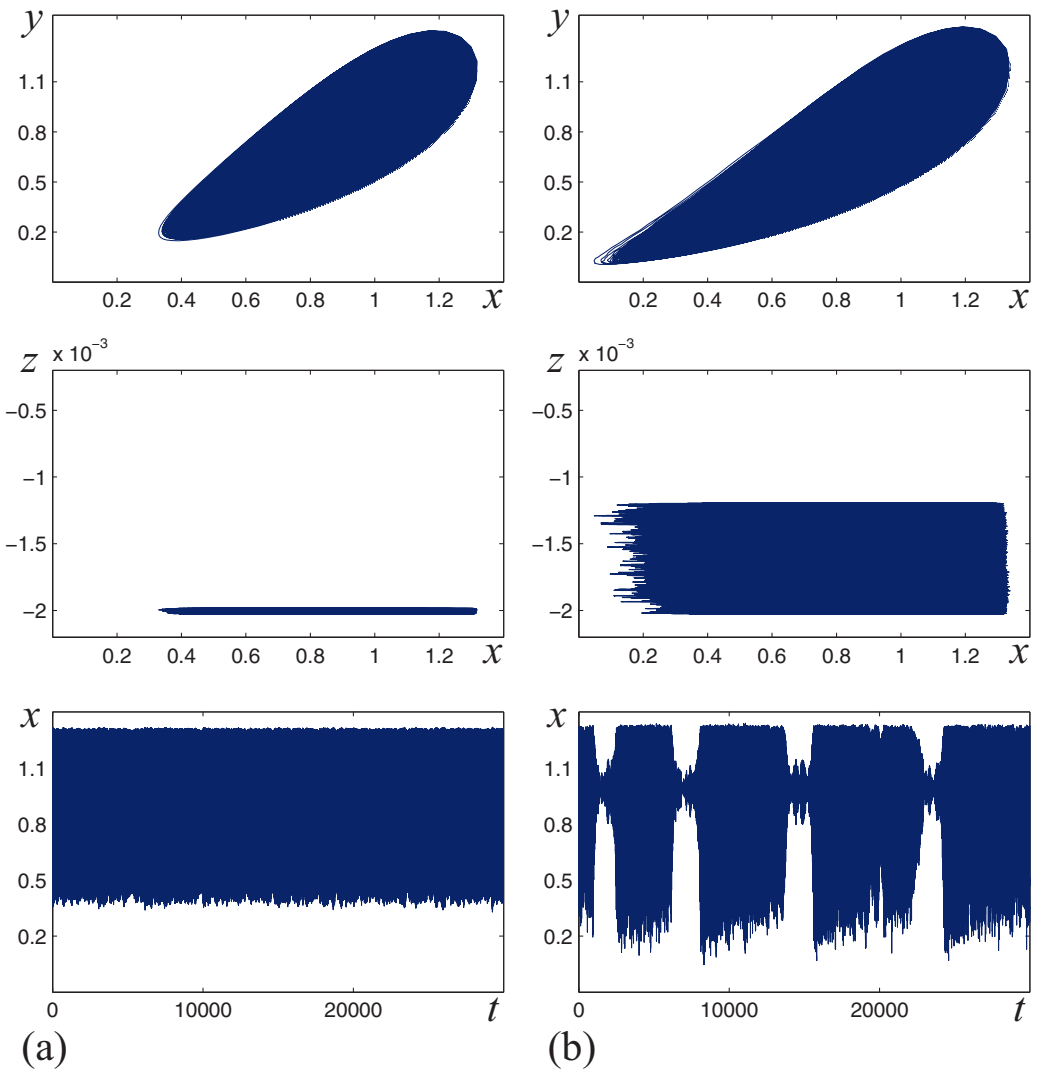

FIG. 4. Stochastic trajectories (in projection on xOy and xOz planes) and corresponding time series $x(t)$ for $\beta = -0.15$: (a) $\varepsilon = 0.001$ and (b) $\varepsilon = 0.005$.

the random trajectories starting from this deterministic cycle and the corresponding time series $x(t)$ for two values of the noise intensity. For a relatively small noise intensity value ($\varepsilon = 0.0001$), random trajectories are concentrated in a small vicinity of the deterministic limit cycle, and the neuron still essentially exhibits tonic spiking, except that this occurs in a noisy fashion [see Fig. 3(a)]. For a greater noise intensity ($\varepsilon = 0.0004$), random trajectories deviate far from the limit cycle and form a structure similar to a torus [see Fig. 3(b)]. On the $x(t)$ plot, one can observe the alternation of large-amplitude

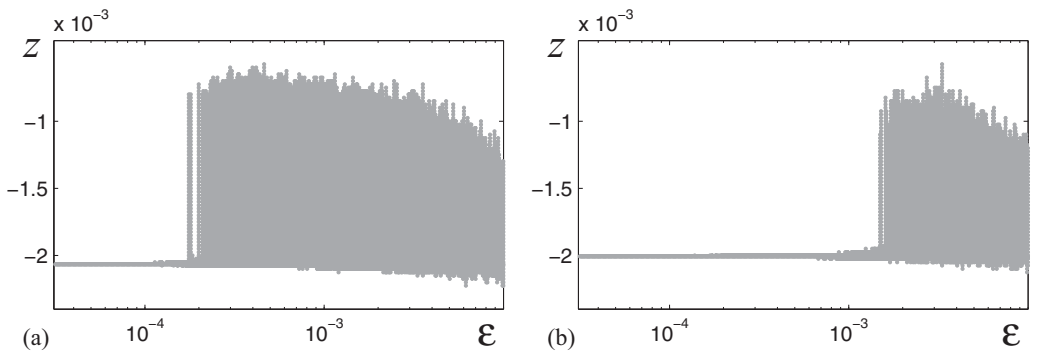

FIG. 5. Noise-induced torus bursting: z coordinates of stochastic trajectories for (a) $\beta = -0.159$ and (b) $\beta = -0.15$.

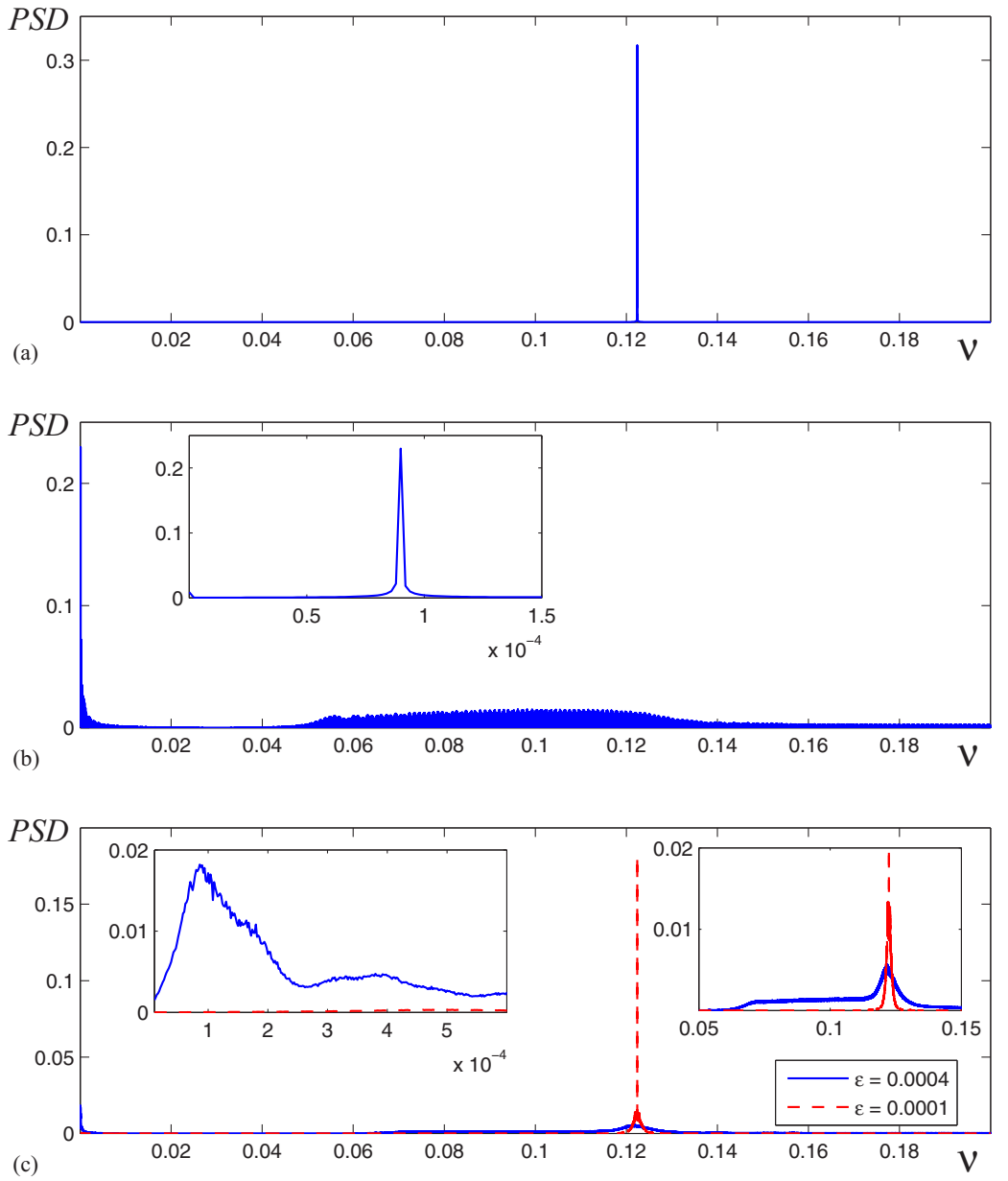

FIG. 6. Power spectral density for (a) $\beta = -0.159$, $\varepsilon = 0$ (deterministic limit cycle); (b) $\beta = -0.162$, $\varepsilon = 0$ (deterministic torus); and (c) $\beta = -0.159$ ($\varepsilon = 0.0001$ and 0.0004).

spiking oscillations and small-amplitude fluctuations near the unstable equilibrium. This indicates that in the presence of noise, oscillations changed from tonic spiking to bursting.

Consider the parameter value $\beta = -0.15$. Figure 4 shows the random trajectories starting from the deterministic limit cycle and the corresponding time series $x(t)$ for two values of the noise intensity. One can observe that for a sufficiently small noise ($\varepsilon = 0.001$), random trajectories are located near the deterministic limit cycle, and this corresponds to the spiking activity. For a greater noise intensity value ($\varepsilon = 0.005$), the stochastic torus is formed, and the type of oscillations can be considered as noisy bursting.

Thus, in the parametric zone $\beta > \beta_2$, where the limit cycle is the attractor of the deterministic system (1), random disturbances form a new dynamical structure resembling a torus, and the dynamical regime changes from spiking to bursting. Let us refer to the regime observed for small noise intensity values as cycle-type stochastic oscillations (CSO). We will refer to the new regime, formed under the noise of sufficiently large intensities, as torus-type stochastic oscillations (TSO).

Let us study the details of the transition from CSO to TSO by examining the changes of the distribution of random trajectories under increasing noise. Figure 5 shows z coordinates of stochastic trajectories for $\beta = -0.159$ and -0.15 depending on the noise intensity. For small noise intensities, random states are localized near the deterministic limit cycle, and they have a sufficiently small dispersion. With an increase of noise, the dispersion of random states grows abruptly. This corresponds to the emergence of TSO. Note that

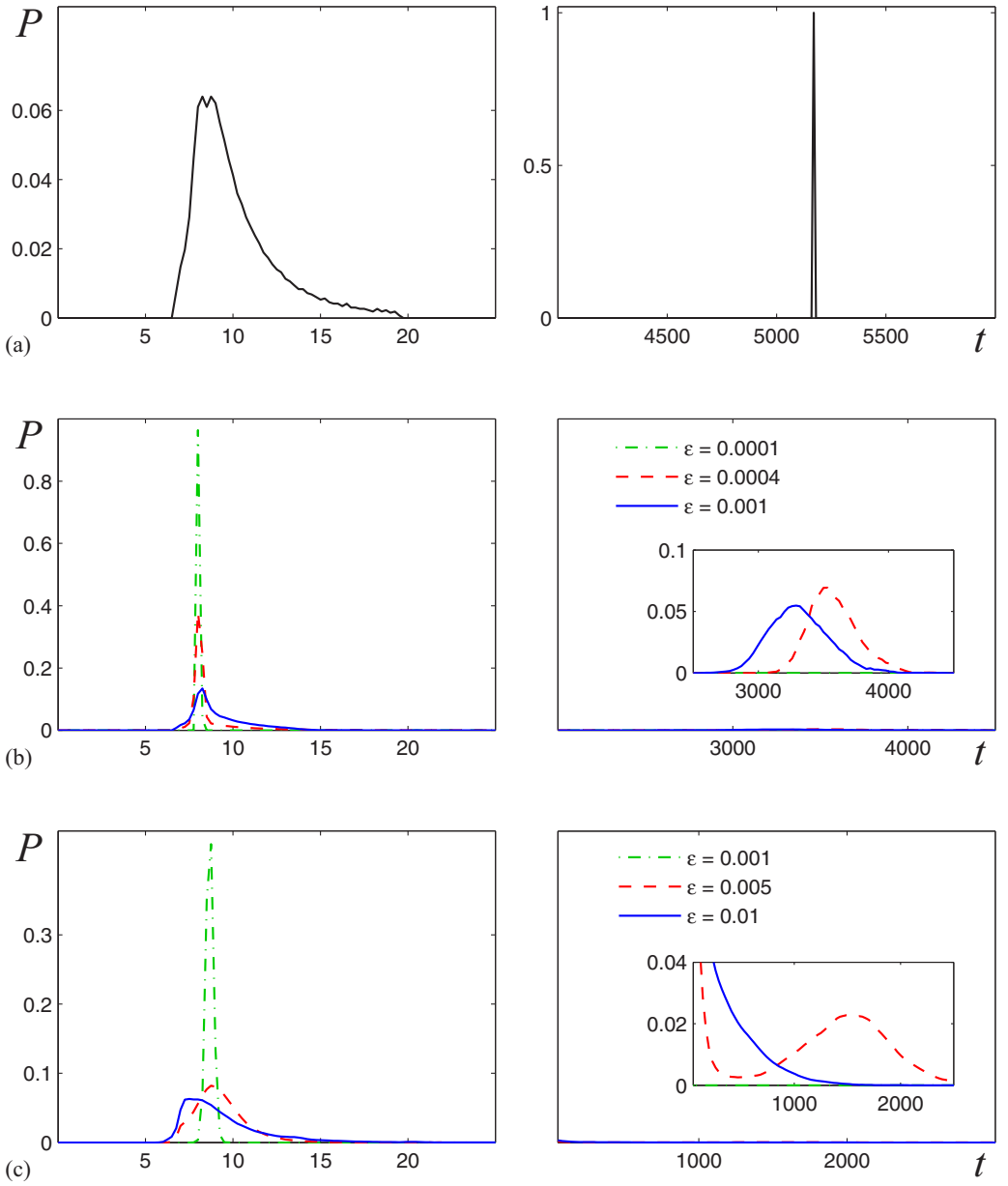

FIG. 7. ISI PDFs for (a) $\beta = -0.162$ ($\varepsilon = 0$), (b) $\beta = -0.159$, and (c) $\beta = -0.15$.

for the value $\beta = -0.159$, which is closer to the bifurcation point β_2, the generation of TSO is observed for smaller values of noise intensity than for $\beta = -0.15$.

The magnitude of the dispersion of random trajectories can be considered as a spacial characteristic for noise-induced torus bursting. To further characterize the temporal features of TSO, we estimate the power spectral density (PSD) of oscillations. In this regard, Fig. 6 shows the PSD for the deterministic attractors (limit cycle and torus). Figures 6(a) and 6(b) show the PSD for $\beta = -0.159$ (deterministic limit cycle) and $\beta = -0.162$ (deterministic torus). For $\beta = -0.159$, the PSD has a single peak corresponding to the frequency of the tonic spiking oscillations: $\nu \approx 0.12$ Hz [see Fig. 6(a)]. The frequency distribution for bursting (torus) oscillations in the HR model is more complicated. The PSD for $\beta = -0.162$ has a peak at $\nu \approx 0.0001$ Hz. This matches the interburst frequency (corresponding to the long interburst period). There is also a significant power at a wide interval of higher frequencies $0.05 < \nu < 0.15$, which corresponds to the rapid spiking oscillations in the active phase of the burst [see Fig. 6(b)].

Let us examine how noise changes the PSD for the limit cycle (tonic spiking regime) for $\beta = -0.159$. For a small noise intensity ($\varepsilon = 0.0001$), the PSD has a single slightly widened peak at the frequency $\nu \approx 0.12$ Hz [see Fig. 6(c)]. This corresponds to a noisy spiking regime. With an increase of the noise intensity ($\varepsilon = 0.0004$), a new additional peak at low frequencies appears ($\nu \approx 0.0001$ Hz), and the peak at higher frequencies expands further. This indicates the noise-induced transformation from the tonic spiking oscillation regime to the torus bursting one.

It is helpful to further analyze the temporal characteristics of stochastic oscillations with the aid of interspike interval (ISI)

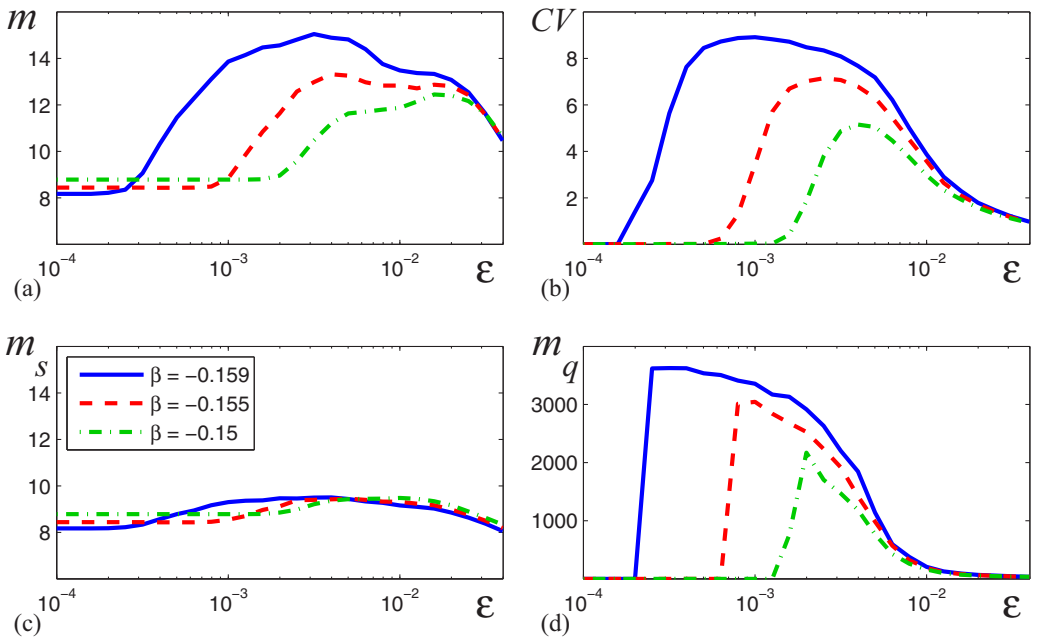

FIG. 8. ISI statistics: (a) mean value (overall), (b) coefficient of variation (overall), (c) mean value (in burst), and (d) mean quiescence interval, for $\varepsilon = -0.159$ (blue solid line), $\varepsilon = -0.155$ (red dashed line), and $\varepsilon = -0.15$ (green dash-dotted line).

statistics. An estimation of interspike interval τ distribution is a common method to study stochastic changes in the oscillatory dynamics of neuron models. Accordingly, to characterize the ISI statistics, we can estimated the ISI probability density function (PDF), the mean value $m = \langle\tau\rangle$, and the coefficient of variation $CV = \frac{\sqrt{\langle(\tau-m)^2\rangle}}{m}$.

A phenomenon of TSO is confirmed by changes of ISI PDFs displayed in Fig. 7 for a different parameter β and noise intensity ε values. Consider $\beta = -0.159$. For a small noise ($\varepsilon = 0.0001$), the ISI PDF is unimodal with the peak corresponding to the period of the limit cycle: $T \approx 8.17$ [see Fig. 7(b)]. With an increase of noise ($\varepsilon = 0.0004$), the PDF becomes bimodal: one can observe a new peak of the ISI PDF in the zone of long ISIs ($\tau \approx 3500$). The emergence of long ISIs indicates the noise-induced transition to the bursting regime (a long interval accounts for a quiescence phase). With a further increase of noise ($\varepsilon = 0.001$), the peak in the zone of long ISIs shifts to the left (thus, the quiescence intervals shorten). Random disturbances also induce changes of probability distribution in the zone of short ISIs: a form of the probability function becomes similar to that of the deterministic torus [see Fig. 7(a) for $\beta = -0.162$]. A similar transformation of the ISI PDF occurs also for $\beta = -0.15$ [see Fig. 7(c)], which indicates the noise-induced transition to the bursting regime. The change of the PDF from unimodal form to bimodal indicates P bifurcation [36] related to the qualitative change of the distribution of ISIs for the stochastic cycle.

Figure 8 shows the overall mean value m [Fig. 8(a)] and the overall coefficient of variation CV [Fig. 8(b)] of ISIs, the mean ISI value within bursts m_s [Fig. 8(c)], and the mean quiescence (interburst) interval m_q [Fig. 8(d)] for different parameter β values under variation of noise intensity. One can observe that for small noise, the overall mean ISI is almost constant and corresponds to the period of the spiking limit cycle. An increase in the noise intensity causes an abrupt rise of the overall mean ISI due to the emergence of long ISIs corresponding to the quiescence phase in the bursting regime. The plots of the overall CV display anticoherence (an increase of variability of ISIs under random disturbances). This is also typical for the bursting dynamics. With a further increase of noise intensity, the variability of ISIs decreases, which corresponds to an increase of system

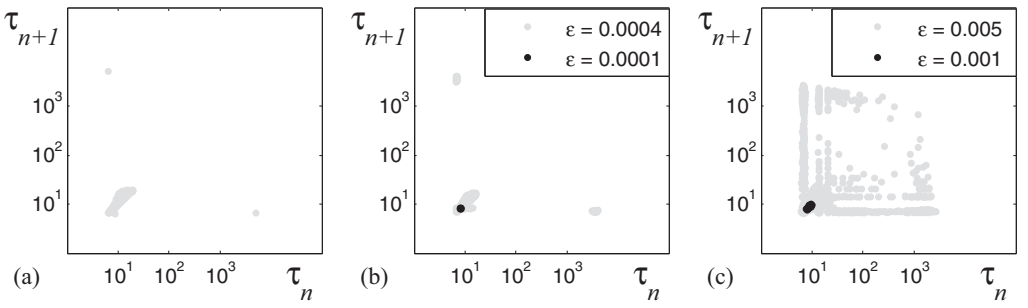

FIG. 9. ISI return maps during noise-induced bursting: (a) $\beta = -0.162$ ($\varepsilon = 0$), (b) $\beta = -0.159$, and (c) $\beta = -0.15$.

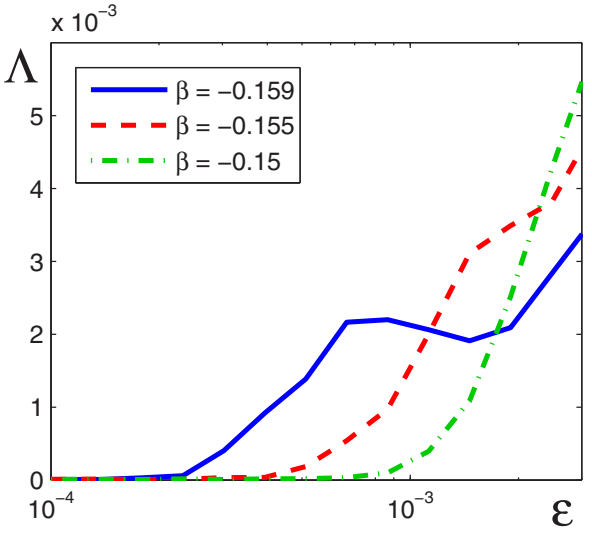

FIG. 10. The largest Lyapunov exponent (LLE) in dependence on the noise intensity.

coherence. Figure 8(c) shows that the mean ISI value within bursts does not significantly change in the presence of noise. In Fig. 8(d), estimations of the quiescence phase duration in the noise-induced bursting regime are displayed. For small noise there are no bursts, and the mean quiescence interval equals zero. With an increase of noise, long ISIs emerge, and this causes a sharp increase of the mean quiescence interval. As noise further increases, the mean interburst interval decreases.

Noise-induced bursting is also clearly demonstrated in return maps of ISIs (i.e., plots of the duration of interval τ_{n+1} versus the duration of the preceding interval τ_n; see Fig. 9). For a small noise, one cluster of ISIs in the bottom left corner of the diagram is observed. This corresponds to the fast spiking dynamics. With an increase of noise, two more clusters of ISIs (in the bottom right and upper left parts of the diagram) appear. Such an ISI return map is typical for the bursting regime: a cluster of ISIs in the bottom left corner of the diagram corresponds to fast spiking inside the bursts, whereas two other clusters refer to the quiescence phases [compare with the ISI return map of the deterministic bursting regime for $\beta = -0.162$, Fig. 9(a)].

Consider finally how TSO in system (2) is mimicked by the behavior of the largest Lyapunov exponent (LLE). Recall that the LLE is a standard quantitative characteristic of the dynamic peculiarities of flows. A negative LLE denotes that the trajectories of the stochastic system mostly converge. Positive values of the LLE instead mark that the divergence dominates. Thus, a change of the sign of the LLE from negative to positive indicates a transformation from regular to chaotic dynamics [37,38].

Figure 10 shows LLEs [$\Lambda(\varepsilon)$] for various β values from the zone of tonic spiking depending on noise intensity. It can be seen that for relatively small values of noise intensity, $\Lambda(\varepsilon) = 0$, and with the increase of noise, the exponent Λ becomes positive. This coincides with the occurrence of a D bifurcation [36] underpinning the qualitative change in the dynamics of the stochastic flow and noise-induced chaos.

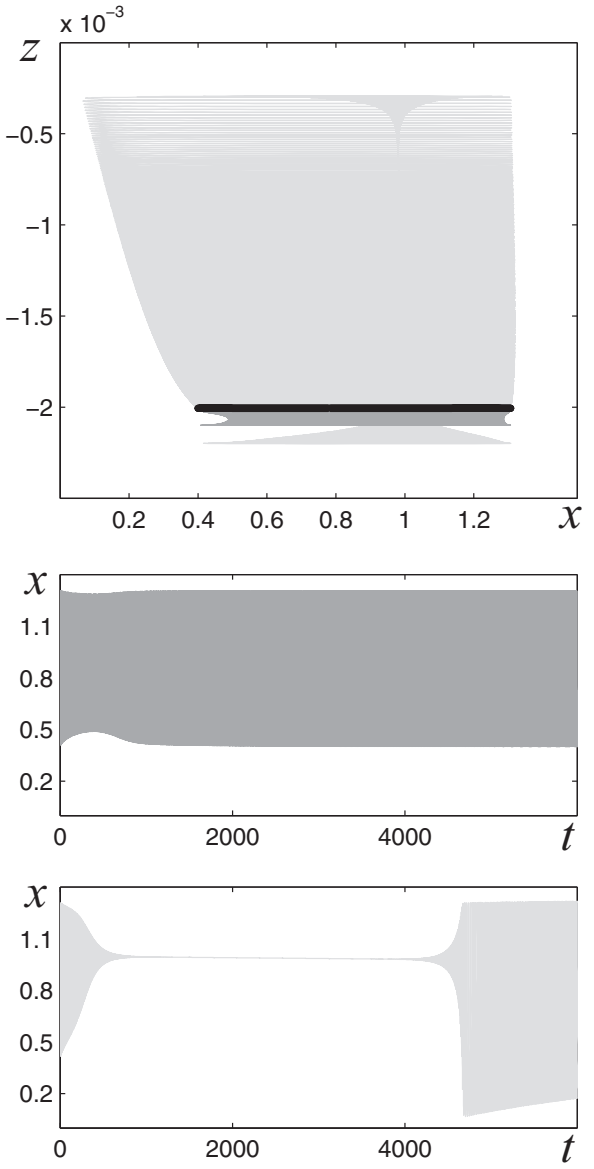

FIG. 11. Deterministic limit cycle (black) and phase trajectories (light gray and dark gray) starting from different initial points for $\beta = -0.15$ with corresponding time series $x(t)$.

In summary, Figs. 5, 8, and 10 allow us to make empirical estimations for critical values of the noise intensity (ε^*) corresponding to the transition from the spiking regime to the bursting one. This transition is characterized by (i) the sharp growth of z-coordinate dispersion, (ii) the increase of the ISI mean value, (iii) the growth of the variation of ISIs, and (iv) the change of the sign of the LLE, which appears at some level of noise. For $\beta = -0.159$ we get $\varepsilon^* \approx 0.0003$, while for $\beta = -0.15$ we have $\varepsilon^* \approx 0.002$.

IV. STOCHASTIC SENSITIVITY ANALYSIS OF NOISE-INDUCED TORUS BURSTING

The emergence of the torus type of stochastic oscillations is related to the peculiarities of the geometrical arrangement of

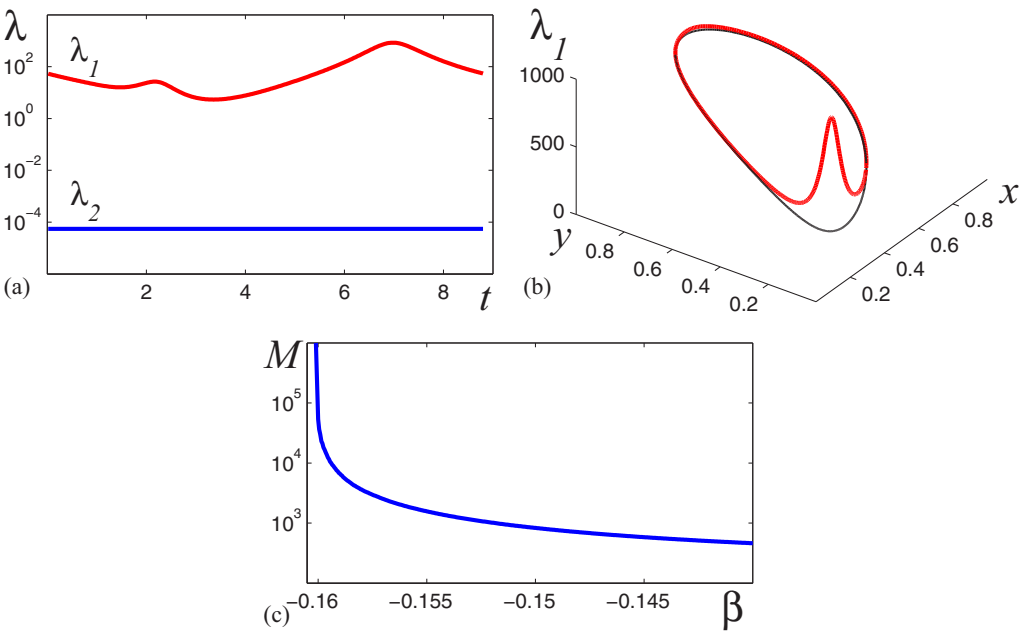

FIG. 12. Stochastic sensitivity of limit cycles: (a) nonzero eigenvalues $\lambda_{1,2}(t)$ of the stochastic sensitivity matrix for $\beta = -0.15$, (b) maximal eigenvalue $\lambda_1(t)$ (red thick solid) along the limit cycle (black thin solid) for $\beta = -0.15$, and (c) stochastic sensitivity factor in the zone of tonic spiking limit cycles.

deterministic trajectories near the limit cycle and its stochastic sensitivity.

Figure 11 shows the deterministic trajectories starting from different points in the vicinity of the limit cycle for $\beta = -0.15$. The trajectories tend to the stable cycle, but the character of this movement can be different. One can determine two types of transient regimes in the phase space. In the first type, the trajectory tends to the limit cycle monotonically. In the second type of transient, the trajectory first goes far from the limit cycle, spends a long time in the vicinity of the unstable equilibrium, and then makes a long approach to the cycle. The type of transient regime depends on the location of the initial point. Thus, there is some border surface between these transient regimes in the phase space. Let us define this border by the term "pseudoseparatrix."

The behavior of the system in the presence of random disturbances is also influenced by the stochastic sensitivity of attractors. To pursue analysis of TSO emergence, we use the technique of stochastic sensitivity functions (SSFs). The mathematical details can be found in the Appendix.

The sensitivity of a stable limit cycle to noise is characterized by the stochastic sensitivity function $W(t)$. In Fig. 12(a), the nonzero eigenvalues $\lambda_{1,2}(t)$ of the matrix function $W(t)$ for $\beta = -0.15$ are plotted. One can observe that the stochastic sensitivity varies nonuniformly along the cycle. The maximum of the SSF (the maximal value of the largest eigenvalue λ_1) corresponds to the part of the cycle with small x coordinates [see Fig. 12(b)].

To determine the stochastic sensitivity of the cycle as a whole, the stochastic sensitivity factor M can be used (see the Appendix). In Fig. 12(c), the stochastic sensitivity factor $M(\beta)$ for limit cycles in the zone $\beta \in (-0.1603, -0.14)$ is plotted. One can observe that as the parameter β approaches the point $\beta = -0.1603$ where the system undergoes the

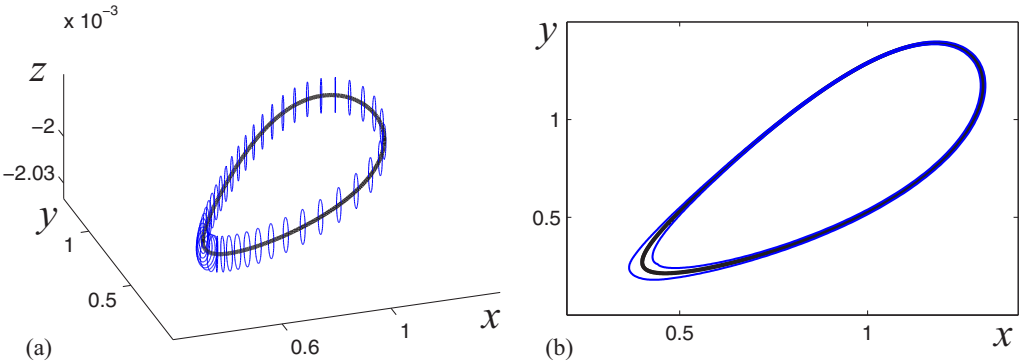

FIG. 13. Set of confidence ellipses (confidence torus) around the deterministic limit cycle (black thick solid) for $\beta = -0.15$ and $\varepsilon = 0.0005$ with fiducial probability $P = 0.99$: (a) in xyz space, (b) in projection on the xOy plane.

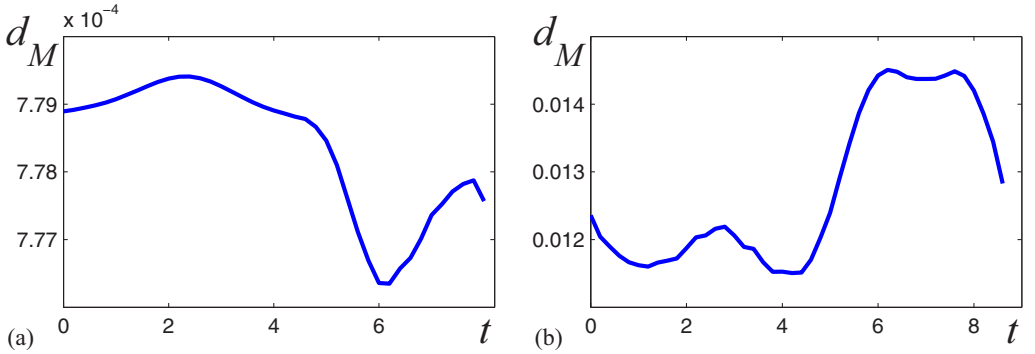

FIG. 14. Mahalanobis distance from the cycle to the pseudoseparatrix for (a) $\beta = -0.159$ and (b) $\beta = -0.15$.

Neimark-Sacker bifurcation, the sensitivity of the limit cycle grows unlimitedly.

The SSF technique allows us to approximate the geometry of a bundle of stochastic trajectories around the deterministic limit cycle. Consider a hyperplane Π_t that is orthogonal to the limit cycle at the point $\bar{x}(t)$. Eigenvalues and eigenvectors of the SSF matrix $W(t)$ define a confidence ellipse located in the plane Π_t. A set of these ellipses for all points $\bar{x}(t)$ forms in the 3D space a confidence torus around the limit cycle. Random trajectories are located entirely inside this confidence torus with the fiducial probability P. Figure 13 shows the confidence torus (a set of confidence ellipses) around the deterministic limit cycle for $\beta = -0.15$, and $\varepsilon = 0.0005$ with fiducial probability $P = 0.99$.

In the generation of TSO, the distance between the deterministic cycle and the pseudoseparatrix plays an important role. For this purpose, the Mahalanobis distance,

$$d_M(x,\bar{x}(t)) = \sqrt{[x-\bar{x}(t)]^\top W^+(t)[x-\bar{x}(t)]},$$

can be used insofar as it takes into account both the geometry of the attractors and their stochastic sensitivity, while being proportional to the probability of escape from a basin of attraction.

Figure 14 shows the plots of the Mahalanobis distance from points of the limit cycle to the pseudoseparatrix for $\beta = -0.159$ and -0.15. The Mahalanobis distance is related to the residence time of the system in the part of the phase space isolated by the pseudoseparatrix surface: the larger the Mahalanobis distance is, the longer is the residence time in this region. Thus, the Mahalanobis metrics allows us to find the "transition zone," i.e., a part of the cycle from which the random trajectories go off to the zone of the phase space outside the pseudoseparatrix surface. This is the part of the cycle where the Mahalanobis distance to the pseudoseparatrix is minimal.

Let us consider the mutual position of the confidence torus and pseudoseparatrix under different noise intensities. Consider the point of the limit cycle from the transition zone and a plane orthogonal to the limit cycle at this point. Let us construct the pseudoseparatrix line, which is an intersection of the pseudoseparatrix surface with the considered plane, and confidence ellipses in this plane. Figure 15 displays a point of cycle from the transition zone, the pseudoseparatrix for $\beta = -0.159$ and -0.15, and the confidence ellipses for different noise intensities. For sufficiently small noise intensity, a confidence ellipse is close to the deterministic cycle. With an increase of the noise intensity, the ellipse expands and intersects the pseudoseparatrix. This means that with high probability, stochastic trajectories can go to the zone of the phase space where they form a stochastic torus. The noise intensity that corresponds to the intersection of the confidence ellipse with the pseudoseparatrix can be used to estimate the critical value ε^*. Note that the point where the confidence ellipse touches the pseudoseparatrix corresponds

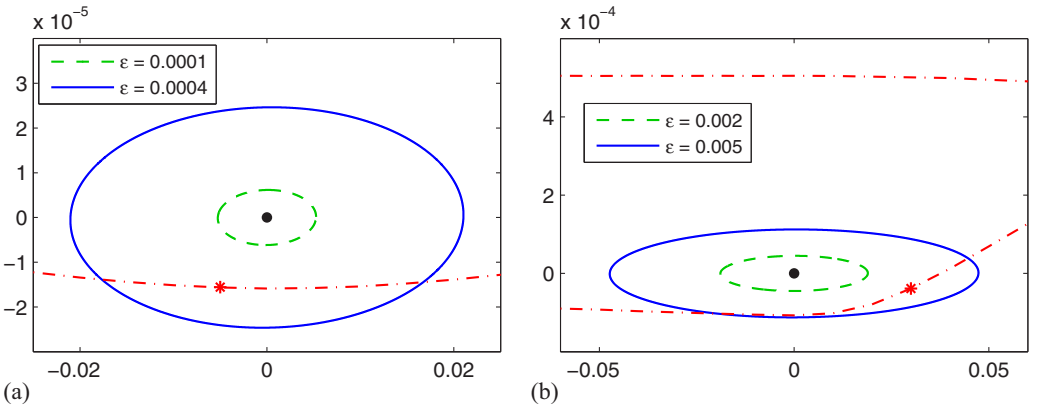

FIG. 15. Point of the limit cycle (black circle), confidence ellipses (solid and dashed lines) with fiducial probability $P = 0.99$, pseudoseparatrix (red dash-dotted line), point of the minimal Mahalanobis distance from cycle to pseudoseparatrix (red asterisk) for (a) $\beta = -0.159$ (for point $t = 6$) and (b) $\beta = -0.15$ (for point $t = 4.2$).

to the minimal Mahalanobis distance. For $\beta = -0.159$ we estimate $\varepsilon^* \approx 0.0003$, and for $\beta = -0.15$ we get $\varepsilon^* \approx 0.003$. These values are in good agreement with the results from our numerical simulations.

V. CONCLUSION

Neural activity is known to have a variety of oscillatory regimes. Along with traditionally considered periodic regimes, more complex ones are observed. Torus bursting takes an important place among them [6,7,9]. A challenging problem is to analyze mechanisms of noise-induced torus bursting. In this paper, the phenomenon of stochastic generation of a torus in the Hindmarsh-Rose neuron model was discovered. We showed that in this model, random disturbances can transform the tonic spiking regime to the torus bursting one. This phenomenon was confirmed by the changes of dispersion of random trajectories as well as the transformation of the power spectral density, and the interspike interval statistics. Qualitative changes of the probability density function (P bifurcations) of the distribution of the interspike intervals were demonstrated. We found that the emergence of torus-type stochastic oscillations is related to the peculiarities of the geometrical arrangement of deterministic trajectories near the limit cycle. Indeed, one can determine two types of transient processes depending on the initial deviation from the limit cycle. For the detailed parametric study of the noise-induced torus bursting mechanism, we applied the approach based on the stochastic sensitivity functions technique, confidence domains, and Mahalanobis metrics methods. With the help of Lyapunov exponents, we showed that the noise-induced torus bursting is accompanied by the stochastic D bifurcation of the transition from order to chaos.

ACKNOWLEDGMENT

The work was supported by the Russian Science Foundation (Russia), Grant No. 16-11-10098.

APPENDIX: STOCHASTIC SENSITIVITY FUNCTION TECHNIQUE

Consider a general nonlinear system of stochastic differential equations:

$$dx = f(x)\,dt + \varepsilon\sigma(x)\xi(t). \tag{A1}$$

Here, x is an n vector, $f(x)$ is a smooth n-dimensional function, $\xi(t)$ is an n-dimensional white Gaussian noise with $\langle \xi(t)\xi^\top(t+\tau)\rangle = \delta(\tau)I$, I is an $n \times n$ identity matrix, $\sigma(x)$ is an $n \times n$ matrix function, and ε is a scalar parameter for the noise intensity. Let the corresponding deterministic system ($\varepsilon = 0$) have an exponentially stable limit cycle Γ, defined by a T-periodic solution $\bar{x}(t) = \bar{x}(t+T)$. Trajectories of the randomly forced system (A1) leave the deterministic cycle Γ and form some probabilistic distribution around it. The time evolution of this distribution is governed by the Kolmogorov-Fokker-Planck (KFP) equation. At steady state, one can consider the stationary probability density function $\rho(x,\varepsilon)$, which is the solution of the stationary KFP equation. This function, however, is often not derivable analytically in multidimensional ($n \geqslant 2$) systems, therefore various approximations and asymptotics are developed [21,39,40]. Here, a well-known quasipotential method [41,42] and a stochastic sensitivity function (SSF) technique [30,33,34] can be applied.

Let Π_t be a hyperplane (or Poincaré section) that is orthogonal to the cycle at the point $\bar{x}(t)\,(0 \leqslant t < T)$. For this plane, in the neighborhood of the point $\bar{x}(t)$, a Gaussian approximation of the stationary probabilistic distribution can be written [33] as

$$\rho_t(x,\varepsilon) = K \exp\left(-\frac{[x-\bar{x}(t)]^\top W^+(t)[x-\bar{x}(t)]}{2\varepsilon^2}\right),$$

where $\bar{x}(t)$ denotes the mean value of x, and $D(t,\varepsilon) = \varepsilon^2 W(t)$ is the covariance matrix. Here the matrix function $W(t)$ is singular, and the sign "+" denotes a pseudoinversion. In particular, $W(t)$ is the unique solution of the boundary value problem [33],

$$\dot{W} = F(t)W + WF^\top(t) + P(t)S(t)P(t) \tag{A2}$$

with conditions

$$W(T) = W(0), \quad W(t)r(t) = 0,$$

where

$$F(t) = \frac{\partial f}{\partial x}(\bar{x}(t)), \quad S(t) = G(t)G^\top(t), \quad G(t) = \sigma(\bar{x}(t)),$$

$$r(t) = f(\bar{x}(t)), \quad P(t) = P_{r(t)}, \quad P_r = I - \frac{rr^\top}{r^\top r}.$$

The matrix function $W(t)$ can be regarded as a measure of stochastic sensitivity of the system to random perturbations, and for this reason it is referred to as the "stochastic sensitivity function" (SSF) for the system (A1). The eigenvalues $\lambda_i(t)$ and the eigenvectors $v_i(t)$ of the SSF matrix characterize the dispersion of random states in the Poincaré section Π_t near the point $\bar{x}(t)$ of the cycle. The value $M = \max_{[0,T]} \lambda_1(t)$ is a useful characteristic of the cycle as a whole. We consider M as a stochastic sensitivity factor of the limit cycle Γ.

The SSF allows us to construct a confidence ellipse with the center in the point $\bar{x}(t)$. The equation of such an ellipse in the plane Π_t reads

$$[x-\bar{x}(t)]^\top W^+(t)[x-\bar{x}(t)] = 2k^2\varepsilon^2,$$

where the parameter k determines a fiducial probability $P = 1 - e^{-k}$. A set of these ellipses for $t \in [0;T)$ specifies some confidence torus around a deterministic cycle. This torus is a confidence domain in a phase space for the stochastic cycle as a whole [34].

[1] E. M. Izhikevich, *Dynamical Systems in Neuroscience: The Geometry of Excitability and Bursting* (MIT Press, Cambridge, MA, 2007).

[2] J. Rinzel and G. B. Ermentrout, Analysis of neural excitability and oscillations, in *Methods in Neuronal Modeling: From Synapses to Networks*, 2nd ed., edited by C. Koch

and I. Segev (MIT Press, Cambridge, MA, 1998) Chap. 7, p. 251.
[3] R. R. Llinas, Front. Cell. Neurosci. **8**, 320 (2014).
[4] E. Benoit, J.-L. Callot, F. Diener, and M. Diener, Collect. Math. **31**, 37 (1981).
[5] J. Guckenheimer, SIAM J. Appl. Dyn. Syst. **9**, 138 (2010).
[6] M. A. Kramer, R. D. Traub, and N. J. Kopell, Phys. Rev. Lett. **101**, 068103 (2008).
[7] J. Burke, M. Desroches, A. M. Barry, T. J. Kaper, and M. A. Kramer, J. Math. Neurosci. **2**, 3 (2012).
[8] A. L. Hodgkin and A. F. Huxley, J. Physiol. **117**, 500 (1952).
[9] G. N. Benes, A. M. Barry, T. J. Kaper, M. A. Kramer, and J. Burke, Chaos **21**, 023131 (2011).
[10] J. L. Hindmarsh and R. M. Rose, Proc. R. Soc. London, Ser. B **221**, 87 (1984).
[11] G. Innocenti, A. Morelli, R. Genesio, and A. Torcini, Chaos **17**, 043128 (2007).
[12] A. Shilnikov and M. Kolomiets, Int. J. Bifurcation Chaos **18**, 2141 (2008).
[13] M. Storace, D. Linaro, and E. de Lange, Chaos **18**, 033128 (2008).
[14] R. Barrio and A. Shilnikov, J. Math. Neurosci. **1**, 6 (2011).
[15] X.-J. Wang, Physica D **62**, 263 (1993).
[16] K. Tsaneva-Atanasova, H. M. Osinga, T. Riess, and A. Sherman, J. Theor. Biol. **264**, 1133 (2010).
[17] J. M. Gonzalez-Miranda, Chaos **13**, 845 (2003).
[18] R. Barrio, M. A. Martinez, S. Serrano, and A. Shilnikov, Chaos **24**, 023128 (2014).
[19] M. Desroches, T. Kaper, and M. Krupa, Chaos **23**, 046106 (2013).
[20] A. S. Pikovsky and J. Kurths, Phys. Rev. Lett. **78**, 775 (1997).
[21] B. Lindner and L. Schimansky-Geier, Phys. Rev. E **60**, 7270 (1999).
[22] B. Lindner, J. Garcia-Ojalvo, A. Neiman, and L. Schimansky-Geier, Phys. Rep. **392**, 321 (2004).
[23] A. Longtin, Phys. Rev. E **55**, 868 (1997).
[24] J. P. Baltanás and J. M. Casado, Phys. Rev. E **65**, 041915 (2002).
[25] A. B. Neiman, T. A. Yakusheva, and D. F. Russell, J. Neurophysiol. **98**, 2795 (2007).
[26] P. Channell, I. Fuwape, A. B. Neiman, and A. L. Shilnikov, J. Comput. Neurosci. **27**, 527 (2009).
[27] P. Hitczenko and G. S. Medvedev, SIAM J. Appl. Math. **69**, 1359 (2009).
[28] I. Bashkirtseva, S. Fedotov, L. Ryashko, and E. Slepukhina, Int. J. Bifurcation Chaos **26**, 1630032 (2016).
[29] I. Bashkirtseva and L. Ryashko, Phys. Rev. E **83**, 061109 (2011).
[30] I. Bashkirtseva, A. B. Neiman, and L. Ryashko, Phys. Rev. E **91**, 052920 (2015).
[31] I. Bashkirtseva, L. Ryashko, and E. Slepukhina, Nonlin. Dyn. **82**, 919 (2015).
[32] I. Bashkirtseva, L. Ryashko, and E. Slepukhina, Fluct. Noise Lett. **13**, 1450004 (2014).
[33] I. A. Bashkirtseva and L. B. Ryashko, Math. Comp. Simulat. **66**, 55 (2004).
[34] L. Ryashko, I. Bashkirtseva, A. Gubkin, and P. Stikhin, Math. Comp. Simulat. **80**, 256 (2009).
[35] P. C. Mahalanobis, Proc. Nat. Inst. Sci. India **2**, 49 (1936).
[36] L. Arnold, *Random Dynamical Systems* (Springer-Verlag, Berlin, 1998).
[37] J. B. Gao, S. K. Hwang, and J. M. Liu, Phys. Rev. Lett. **82**, 1132 (1999).
[38] F. Gassmann, Phys. Rev. E **55**, 2215 (1997).
[39] C. Kurrer and K. Schulten, Physica D **50**, 311 (1991).
[40] G. N. Milshtein and L. B. Ryashko, J. Appl. Math. Mech. **59**, 47 (1995).
[41] M. Dembo and O. Zeitouni, *Large Deviations Techniques and Applications* (Jones and Bartlett, Boston, 1995).
[42] M. I. Freidlin and A. D. Wentzell, *Random Perturbations of Dynamical Systems* (Springer, New York, 1984).